Strain Gage Backing Effects on Measuring Steep Strain Gradient

N. T. Younis **and** **B. Kang**

younis@engr.ipfw.edu kang@engr.ipfw.edu

Department of Engineering

Indiana University – Purdue University Fort Wayne

Fort Wayne, Indiana 46805-1499, USA

ABSTRACT

Electric strain gages have been used to obtain average extensional strain over a given gage length since the 1930s. However, the literature regarding the inherent uncertainty in a gradient strain measurement is scarce. The resistive gages are produced as flat foils by printed circuit techniques, in the form of a grid on a plastic backing. The novelty of this research program is to examine the manufacturing of the strain gage by modeling the behavior of the gage. The principal sources of error that influence the measurement of stress concentration factors are studied. Recommendations for manufacturing strain gages for high strain gradient measurements are made.

Keywords: Strain gage backing, strain gradient

INTRODUCTION

The capability of the resistance strain gage for general- purpose stress analysis has been thoroughly demonstrated by its dominance in the field. Thus, recent issues deal with how the accuracy is affected by operational and environmental variables. The theoretical errors caused by thermal effects and gage factor data given by the manufacturers were studied by Cappa [1].

Zubin [2] carried out a theoretical error investigation of calibration beams used for the determination of the gage factor. Impedance strain gage characteristics and enhancing the electromagnetic properties that would contribute to the high signal to noise ratio detection were reported by researchers in the magnetic technology field [3]. The local reinforcement effect in tension is studied by using a simple theoretical model by considering a strain gage mounted on a semi-infinite plate having the same width of the strain gage and subjected to a uniaxial tension load [4]. A computer simulation of strain gage thermal effects error during residual stress hole drilling measurements is presented in reference [5]. To overcome the issues of traditional structural health monitoring, a wireless system was used for strain measurements in which a voltage link transceiver unit was locally connected to the strain gages [6]. In 2010, a proposal for a thin polysilicon strain gage was presented to enhance the sensitivity of the gage [7]. A mathematical model has been developed for an elongated strip and applied to an advanced ceramic strain gage electrical sensor design. The results obtained can be used to determine the thickness of the gage for a given material and length [8]. Most recently, Montero et al. presented a new methodology for determining the uncertainty in a strain gage measuring system by developing an error model and applying the law of propagation of uncertainty [9]. Younis and Kang researched the filaments effect on integrating the strain by mathematically modeling the averaging effects [10].

Foil strain gages are readily manufactured in a variety of configurations [11]. The bonded wire gage consists of a grid of fine wire filament cemented between two sheets of treated paper or plastic backing (matrix) as shown in Fig. 1. The photoetching process used to create the metal-foil grids is very versatile, enabling a wide verity of gage sizes and grid shapes to be produced. The grid is bonded to a thin plastic backing film or carrier because the foil is fragile. The backing

serves to insulate the grid from the metal surface on which it is to be bonded, and functions also as a carrier so that the filaments can be handled.

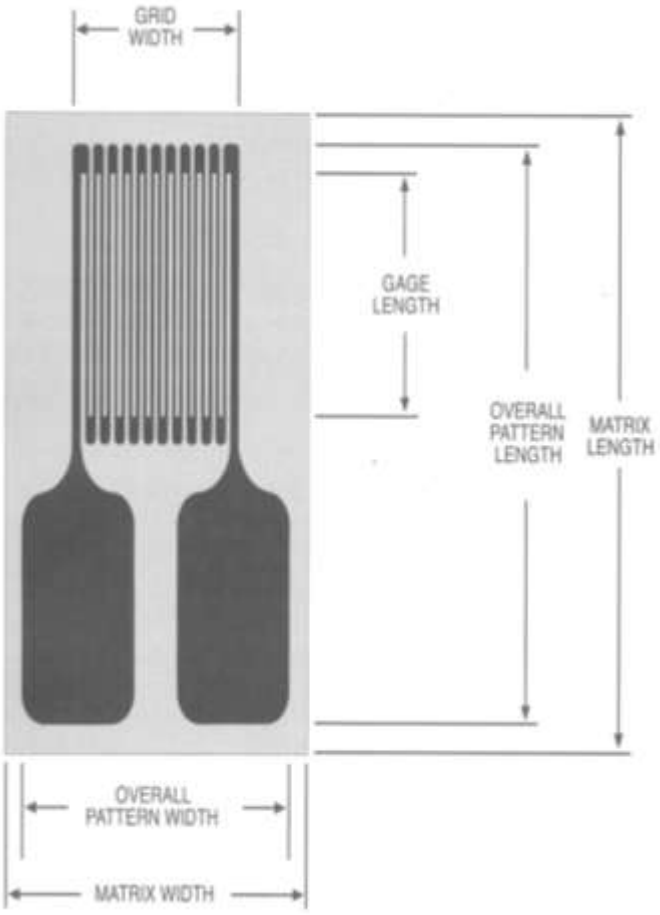

Figure1. Gage dimensions

PROBLEM STATEMENT

This study deals with the manufacturing of the strain gage in regard to high strain gradient measurements. The focus is on the backing and the size of filaments. The mathematical model is based on the parameters shown in Fig. 2. Based on the results obtained for numerous commercial gages, practical manufacturing recommendations are made and selection criterion for the practitioners of experimental stress analysis is outlined.

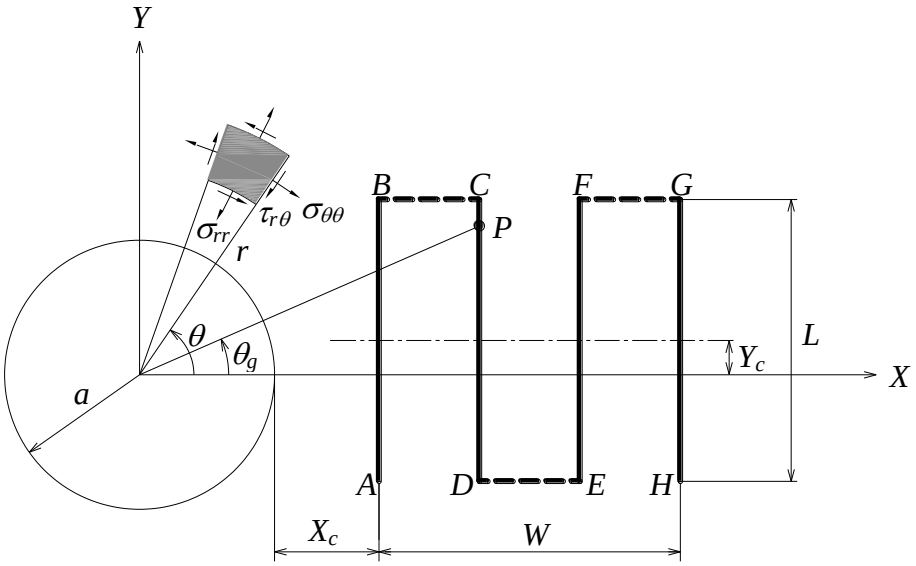

Figure2. Strain gage model and parameters

THEORY

The principal component that determines the operating characteristics of a strain gage is the strain-sensitive alloy used in the foil grid. However, the alloy is not in every case an independently selected parameter because the gage is manufactured as a system. The system consists of a foil and backing combination.

Stress Analysis

A discrete averaging mathematical error model is formulated to study the interaction between the tabs, encapsulation, sensing grid, and strain gradients. To this end, the stress distribution in the vicinity of a circular hole is considered. Kirsch published the elasticity solution for a circular hole in an infinite plate loaded by uniaxial stress [12]. The solution is based on the restrictions of homogeneity, isotropy, and the diameter of the hole is small compared with the width of the

plate but not smaller than the thickness of the plate. For a hole of radius a in a tensile stress field σ_o, the stresses are:

$$\sigma_{\theta\theta} = \frac{\sigma_o}{2}\left(-1 - 3\frac{a^4}{r^4}\right)\cos 2\theta + \frac{\sigma_o}{2}\left(1 + \frac{a^2}{r^2}\right) \qquad (1a)$$

$$\sigma_{rr} = \frac{\sigma_o}{2}\left(1 - 4\frac{a^2}{r^2} + 3\frac{a^4}{r^4}\right)\cos 2\theta + \frac{\sigma_o}{2}\left(1 - \frac{a^2}{r^2}\right) \qquad (1b)$$

$$\tau_{r\theta} = \frac{\sigma_o}{2}\left(-1 - 2\frac{a^2}{r^2} + 3\frac{a^4}{r^4}\right)\sin 2\theta \qquad (1c)$$

Figure 3 shows how the edge tangential stress $\sigma_{\theta\theta}$ varies around the hole. On the boundary of the hole, equations 1b and 1c yield radial stress σ_{rr} equals to shear stress $\tau_{r\theta}$ and both are zero. As shown in Fig. 3, $\sigma_{\theta\theta} = 3\,\sigma_o$ at points A and $\sigma_{\theta\theta} = -\,\sigma_o$ at points B. Thus, the stress concentration factor (SCF) is 3. It is worth mentioning that for a central hole in a finite width plate, the SCF error is less than 5% if the width of the plate is eight times greater than the hole's radius [13].

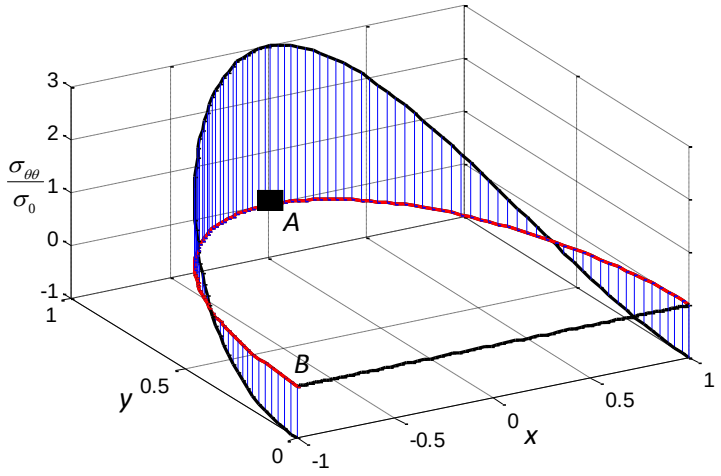

Fig. 3 Edge-tangent stress variation around the hole

The radial σ_{rr}, shear $\tau_{r\theta}$, and the tangential stress distributions are plotted as a function of position away from the boundary of the hole (r = 1.2a) in Fig. 4. This is the region where the strain gage usually mounted. The interaction between these stress gradients is a factor in underestimating the value of the maximum tangential strain by the strain gage.

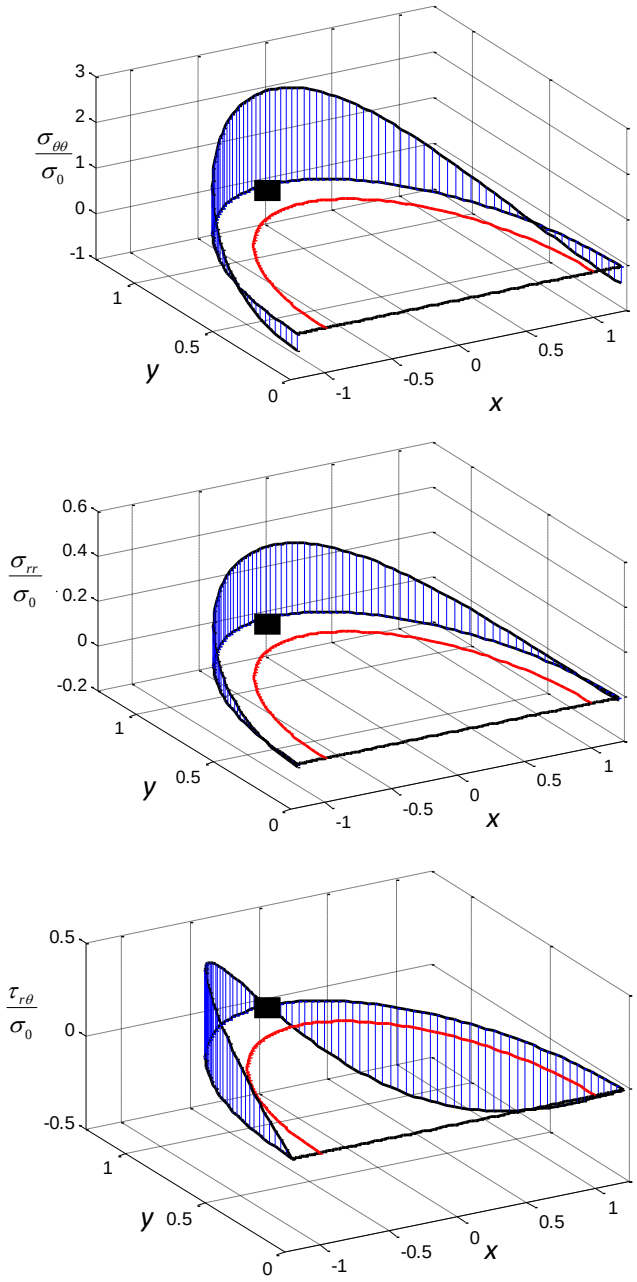

Fig. 4 Tangent, radial, and shear stresses distribution at r = 1.2a.

Strain Gradient

The strain gage reading is dependent on both the radial ϵ_{rr} and tangential $\epsilon_{\theta\theta}$ strains. Utilizing generalized Hooke's laws, one can determine the strains in terms of the mechanical properties of the materials: Young's modulus (E), modulus of rigidity (G), and Poisson's ratio (ν). Thus,

$$\in_{\theta\theta} = \frac{1}{E}(\sigma_{\theta\theta} - \nu\,\sigma_{rr}) \qquad (2a)$$

$$\in_{rr} = \frac{1}{E}(\sigma_{rr} - \nu\,\sigma_{\theta\theta}) \qquad (2b)$$

$$\gamma_{r\theta} = \frac{\tau_{r\theta}}{G} \qquad (2c)$$

Strain gages are rectangular with different aspect ratios. Therefore, it is necessary to mathematically model the strain in rectangular coordinates as:

$$\varepsilon_x = \in_{rr} \cos^2\theta + \in_{\theta\theta} \sin^2\theta - \gamma_{r\theta} \sin\theta \cos\theta \qquad (3a)$$

$$\varepsilon_y = \in_{rr} \sin^2\theta + \in_{\theta\theta} \cos^2\theta + \gamma_{r\theta} \sin\theta \cos\theta \qquad (3b)$$

In practice, the gage is mounted as shown in Fig. 2. Therefore, the strain in the y directions is

$$\varepsilon_y = \frac{\sigma_o}{2E}\left\{(sin^2\theta - \nu cos^2\theta)\left[\left(1 - 4\frac{a^2}{r^2} + 3\frac{a^4}{r^4}\right)\cos 2\theta + \left(1 - \frac{a^2}{r^2}\right)\right]\right\} +$$

$$\frac{\sigma_o}{2E}\left\{(cos^2\theta - \nu sin^2\theta)\left[\left(-1 - 3\frac{a^4}{r^4}\right)\cos 2\theta + \left(1 + \frac{a^2}{r^2}\right)\right]\right\} +$$

$$\frac{\sigma_o}{2E}\left\{(1+\nu)\left[\left(-1 - 2\frac{a^2}{r^2} + 3\frac{a^4}{r^4}\right)\sin^2 2\theta\right]\right\} \qquad (4)$$

The next step is to convert the strain that would be measured by the gage in polar coordinates (r-θ) system to strain in the x-y coordinate system. The coordinates of point P shown in Fig. 2 are x and y and the corresponding coordinates are

$$r = \sqrt{(x^2 + y^2)} \quad \text{and} \quad \theta = \theta_g = \tan^{-1}\frac{y}{x} \qquad (5)$$

The last strain analysis step is to convert the strain along the filaments, yields

$$\epsilon_{y=} \frac{\sigma_o}{2E}\left\{2 - 4\frac{a^2}{r^4}\,y^2 + 3\frac{a^4}{r^4} - \frac{a^2}{r^2} + 2\frac{a^2}{r^4}\left(1 - 6\frac{a^2}{r^2}\right)x^2 + 12\frac{a^4}{r^8}x^4 + \frac{a^2}{r^6}\left(16 - 12\frac{a^2}{r^2}\right)x^2y^2\right\}$$
$$- \frac{\nu\,\sigma_o}{2E}\left\{\frac{a^2}{r^2} - 3\frac{a^4}{r^4} + 6\frac{a^2}{r^4}\left(2\frac{a^2}{r^2} - 1\right)x^2 + \frac{a^2}{r^6}\left(8 - 12\frac{a^2}{r^2}\right)x^4 + \frac{a^2}{r^6}\left(12\frac{a^2}{r^2} - 8\right)x^2y^2\right\} \quad (6)$$

Mathematical Modeling

The discrete averaging effects of a strain gage along the gage filaments are taken into account in the assessment of the errors due to the backing effect. In the data presented it is assumed that the gage is mounted perfectly at the edge of the hole. Due to the difference between the matrix and grid sizes, the distance between the hole's edge and the first filament is X_c as shown in Fig. 2. The average strain (ϵ_{avg}) is also a function of the gage width W, length L_g, and lateral displacement Y_c. For computational purposes, it is advantageous to compare the size and location of the gage to the hole radius *a*, hence the gage parameters are normalized against the radius of the hole. Hence,

$$\varepsilon_{avg} = f\left(\frac{W}{a}, \frac{L}{a}, \frac{X_c}{a}, \frac{Y_c}{a}, n\right) = f(w, l, x_c, y_c, n) \qquad (7)$$

Therefore, the average strain experienced by a strain gage with *n* filaments placed in the *y*-direction can be determined from

$$\varepsilon_{avg} = \frac{1}{nl_g} \sum_{k=1}^{n} \int_{y_c - l_g/2}^{y_c + l_g/2} \varepsilon_{yk} dy \qquad (8)$$

where the ε_{yk} denotes the strain in the k^{th} filament that can be found by

$$\varepsilon_{yk}(x,y) = \begin{cases} \varepsilon_y(1 + x_c, y) & \text{for } n = 1 \\ \varepsilon_y(1 + x_c + \dfrac{(k-1)w}{n-1}, y) & \text{for } n \geq 2 \\ & \text{and } (k = 1, 2, \cdots, \leq n) \end{cases} \qquad (9)$$

The integral in Eq. (9) can be readily evaluated using various numerical integration algorithms. The percentage error of measuring the actual maximum strain (ϵ_{act}) can be calculated as

$$Error = \left(1 - \frac{\varepsilon_{avg}}{\varepsilon_{act}}\right) x\ 100 \qquad (10)$$

RESULTS

The metallic strain gage consists of a metallic foil arranged in a grid pattern. The grid pattern maximizes the amount of metallic wire or foil subject to strain in the parallel direction. The cross-sectional area of the grid is minimized to reduce the effect of shear strain and Poisson's ratio mismatch. The grid is bonded to a thin backing, called the carrier, which is attached directly to the test specimen. Therefore, the strain experienced by the test specimen is transferred directly to the strain gage which can be mathematically computed using equation (9).

Manufacturers offer a wide range of models that may be used for most strain measurement applications. The strain gage manufacturer incorporates durable construction and flexibility into its design criteria, even a "general-purpose" strain gage can be perfectly acceptable for high-accuracy static and dynamic measurement. However, the backing size is a major source of error in measuring strain in steep strain gradient regions. In this study, the gages for most

experimental stress analysis applications are considered. Table 1 shows the dimensions of these gages, the number of the filaments, and percentage error.

DISCUSSION

In most stress analysis situations, the ideal strain gage would change resistance only due to the deformations of the surface to which the sensor is attached. However, the backing materials is not completely an independently specifiable parameter. First, it is assumed that the gage mounted perfectly such that $Y_c=0$. The following conclusions can be made:

1. For a given gage length and width, the error resulting from the backing size (X_c) is very high.
2. Selecting gages that have the same length, the error in measuring the actual strain due to backing size is greater than the one resulting from the gage width.
3. For a constant gage width, the predominant source of error is the distance X_c from the point with the maximum strain to the first filament.

Table 1 shows the error due to the misalignment of the gage, i.e., $Y_c\neq0$ which is a human factor. This is typical in experimental stress analysis even for an experienced engineer with considerable skill and agility. It is obvious that the gage error increases with a 1 mm misalignment between the hole's x-axis and the gage's horizontal center line. But, this error increase is small compared to a 1 mm shift from the hole's edge to the first filament (X_c).

Table 1- Error due to the backing of strain gages

Gage Length (mm)	Grid width (mm)	Matrix width (mm)	Xc (mm)	n	Error (%)	
					Yc = 0 (mm)	Yc = 1 (mm)
0.38	0.51	3.0	1.245	12	42.8	44.5
0.38	0.51	4.6	2.045	10	51.5	51.9
0.79	1.57	4.1	1.265	28	48.7	49.5
0.79	1.57	3.5	0.965	24	45.3	46.6

0.79	0.81	3.0	1.095	14	42.7	44.4
0.79	0.81	5.8	2.495	22	55.5	55.5
0.81	1.52	4.8	1.64	22	51.8	52.3
1.57	1.57	3.6	1.015	18	46.1	47.2
1.57	1.57	4.1	1.265	18	48.8	49.6
1.57	1.57	3.8	1.115	22	47.2	48.2
1.57	1.57	4.6	1.515	20	51.1	51.6
1.57	1.57	7.4	2.915	20	58.8	58.6
1.57	1.57	7.9	3.165	22	59.6	59.4
1.52	1.27	4.32	1.525	20	50.1	50.7
1.57	3.05	4.8	0.875	34	50.3	51.0
3.18	3.18	5.6	1.21	28	53.5	53.8
3.18	3.18	5.6	1.21	14	53.4	53.7
3.18	2.24	5.6	1.66	12	54.1	54.3
3.18	1.57	4.1	1.265	10	49.2	49.8
3.18	1.57	3.3	0.865	20	45.2	46.2
3.18	1.78	4.32	1.27	12	50.0	50.6
3.18	2.54	4.8	1.13	28	51.3	51.8
3.18	4.57	6.9	1.165	32	55.8	56.0
4.75	4.57	6.9	1.165	28	56.0	56.1
6.35	6.35	9.1	1.375	26	58.8	58.8
6.35	3.18	5.6	1.21	20	54.1	54.2
6.35	3.18	5.6	1.21	12	54.1	54.2
6.35	4.45	6.9	1.225	24	56.3	56.3
6.35	2.54	4.32	0.89	10	50.7	51.0
6.35	3.05	5.6	1.275	8	54.1	54.2
6.35	4.57	6.9	1.165	24	56.2	56.2
9.53	4.57	6.9	1.165	18	56.5	56.5
12.7	4.45	7.6	1.575	10	57.8	57.8
12.7	4.57	6.9	1.165	8	56.8	56.9
50.8	4.78	8.1	1.66	8	64.0	64.0

RECOMMENDATIONS

When the carrier matrix (backing) is strained, the strain is transmitted to the grid material through the adhesive. In a strain gage application, the carrier matrix and the adhesive must work together to faithfully transmit strain from the specimen to the grid. However, the backing is a major source of error in measuring peak strains at steep strain gradient areas as shown in table 1. This is due to the fact that a strain gage tends to average the strain over the filaments as well documented in reference [14]. Thus, if a strain gage is manufactured with reducing the distance

between the first sensing filament and SCF point, the error of integrating the strain over the filaments can be minimized as shown in Table 2. In this table, the same gages that are listed in table 1 are considered with the assumption that the backing between the edge of the hole and the sensing gird was removed (Xc = 0). It is obvious that the error in measuring steep strain gradient area is reduced significantly. For example, the percentage error of gage 1 is reduced by more than thirty while for the sixth gage the reduction is about 40%.

CONCLUSIONS

Perhaps the most significant current engineering trend posing a challenge to strain gage practitioners is the measurement of strain where its gradient is quite steep. This study shows that the measurement of strain in steep strain gradients zone utilizing electrical resistance strain gages can be enhanced. The gage tendency of integrating the nonuniform strain distribution is studied and the error would be reduced if the manufacturing of the gage is altered. The results show that if the backing's size is reduced in the vicinity of a stress raiser, the error of measuring steep strain would be reduced by more than 35%. Furthermore, the discrete averaging effects could be reduced if the experimental stress practitioner chooses a gage with very few filaments.

Finally, it is adequate to allow the disadvantages of reducing the backing size to out weight the disadvantages at this stage. These disadvantages are expected to be taken care of with versions of gages that are unsymmetrical.

Table 2 – Results with this study recommendations

Gage Length (mm)	Grid width (mm)	Matrix width (mm)	Error (%)	
			Yc = 0 (mm)	Yc = 1 (mm)
0.38	0.51	3.0	11.5	21.3
0.38	0.51	4.6	11.5	21.3
0.79	1.57	4.1	27.0	32.4
0.79	1.57	3.5	26.9	32.4

0.79	0.81	3.0	17.1	25.1
0.79	0.81	5.8	17.1	25.1
0.81	1.52	4.8	26.4	32.0
1.57	1.57	3.6	27.8	32.8
1.57	1.57	4.1	27.8	32.8
1.57	1.57	3.8	27.8	32.8
1.57	1.57	4.6	27.8	32.8
1.57	1.57	7.4	27.8	32.8
1.57	1.57	7.9	27.8	32.8
1.52	1.27	4.32	24.5	30.2
1.57	3.05	4.8	39.0	41.9
3.18	3.18	5.6	41.5	43.3
3.18	3.18	5.6	41.1	43.1
3.18	2.24	5.6	35.9	38.5
3.18	1.57	4.1	30.9	34.3
3.18	1.57	3.3	31.1	34.4
3.18	1.78	4.32	32.7	35.8
3.18	2.54	4.8	38.1	40.4
3.18	4.57	6.9	46.7	48.0
4.75	4.57	6.9	48.2	48.9
6.35	6.35	9.1	53.0	53.2
6.35	3.18	5.6	45.6	46.1
6.35	3.18	5.6	45.5	46.0
6.35	4.45	6.9	49.3	49.6
6.35	2.54	4.32	43.1	43.7
6.35	3.05	5.6	44.9	45.4
6.35	4.57	6.9	49.6	49.9
9.53	4.57	6.9	51.7	51.8
12.7	4.45	7.6	53.1	53.2
12.7	4.57	6.9	53.2	53.4
50.8	4.78	8.1	63.8	63.8

REFERENCES

1. P. Cappa, Random errors caused by temperature in magnitude of principal strains evaluated with 3-element strain gauge rosettes, Strain, 25 (1989) 139-144.
2. D. Zubin, Theoretical design of calibration beams for strain gauge factor measuring apparatus, Strain, 34 (1998) 99-107.

3. T. Uchiyama and T. Meydan, Impedance strain gauge characteristics of glass covered amorphous magnetic wires, Journal of Optoelectronics and Advanced Materials, 4 (2002) 277-280.
4. A. Ajovalasit and B. Zuccarello, Local reinforcement effect of a strain gauge installation on low modulus materials, The Journal of Strain Analysis for Engineering Design, 40 (2005) 643-653.
5. P. Litos, M. Svantner, and M. Honner, Simulation of strain gauge thermal effects during residual stress hole drilling measurements, The Journal of Strain Analysis for Engineering Design, 40 (2005) 611-619.
6. B. Decker, H. Rasheed, R. Peterman, A. Esmaeily, and H. Melhem, Exploring wireless strain measurement for civil infrastructure, Strain 45 (2009) 547-552.
7. Y. Kim, C. Lee, and S. Kwon, Thin polysilicon gauge for strain measurement of structural elements, Sensors Journal, IEEE, 8 (2010) 1320-1327.
8. E. Suhir, W. Gschohsmann, and J. Nicolcs, Analysis of an elongated stretched strip, with application to a strain-gage electrical sensor design, Journal of Applied Mathematics and Mechanics, 16 (2010) 1-9.
9. W. Montero, R. Farag, V. Diaz, M. Ramirez, and B.L. Boada, Uncertainties associated with strain measuring systems using resistance strain gauges, The Journal of Strain Analysis for Engineering Design, 46 (2011) 1-13.
10. N. T. Younis and B. Kang, Resistance strain gage filaments effect, the Seventh Jordanian International Mechanical Engineering Conference, Amman, Jordan, September 27-29, 2010.
11. Strain Gage Selection: Criteria, Procedures, Recommendations. Strain Gages and Instruments Technical Note, Micro-Measurements, Document Number 11055 (2010).

12. R. D. Cook and W. C. Young, Advanced Mechanics of Materials, second edition, 1999.

13. N. T. Younis, Assembly stress for the reduction of stress concentration, Mechanics Research Communications, 33 (2006), 837-845.

14. N. T. Younis and B. Kang, Averaging effects of a strain gage, Journal of Mechanical Science and Technology, 25 (2011) 163-169.